

Effect of Hydration and Self-Association on the Reaction Mechanism of Proton Transfer in Methimazole: A Theoretical Study

Hossein Roohi,*[1] Setodeh Baghery,[1] and Sayed Gholamreza Hosseini[2]

[1]Department of Chemistry, Faculty of Science, University of Sistan and Baluchestan, P. O. Box 98135-674, Zahedan, Iran

[2]Department of Physiology, Islamic Azad University of Tonkabon, Tonkabon, Iran

Received March 3, 2008; E-mail: hroohi@hamoon.usb.ac.ir

To investigate the effect of hydration and self-association on the reaction mechanism of proton transfer in methimazole (3-methyl-1*H*-imidazole-2(3*H*)-thione) and 1*H*-imidazole-2(3*H*)-thione, quantum chemical calculations were performed at the B3LYP/6-311++G(2d,2p) level of theory. The binding energies of complexes formed in self-assisted reaction are greater than H_2O-assisted reactions. The results show that the thione complexes are more stable than corresponding thiols. The energy barrier for direct proton-transfer tautomerization reaction is significantly greater than self-assisted and H_2O-assisted transfer tautomerization. Direct transition is more difficult than the water-assisted and self-assisted processes both thermodynamically and dynamically. The small negative value of $H(r)$ obtained by AIM analysis at the B3LYP/6-311++G(2d,2p) level reveals some contribution of sharing interaction (partially covalent) to the S···HN bond. AIM data also reveal the partially covalent nature of S···H5 interaction and electrostatic nature of O···H6 interaction in the hydrated complexes. In the present complexes, results obtained by NBO analysis show that there is an increase in the σ^* population of the N–H bond in **A**(**C**) and that of O–H bond in **W** upon dimerization.

Methimazole (MMI) has been the subject of intense research duo to its *anti*-thyroid action. MMI is an *anti*-thyroid agent which depresses the formation of thyroid hormones and, for this reason, is a major drug currently used for the treatment of hyperthyroidism. This drug and other *anti*-thyroid agents bearing the thiourea pharmacophore, inhibit the first step in the pathway of thyroid hormone biosynthesis. It has been proposed that the donor property, i.e. Lewis basicity, of *anti*-thyroid agents bearing the thiourea group is at the origin of their *anti*-thyroid action.[1–6]

Suszka have suggested that both thione and thiol tautomers of MMI are involved in complex formation.[7] Tautomerization of MMI causes the concentration of the thione form of MMI to decrease. Protomeric tautomerization reactions are important in many chemical and biological systems. Laurence et al. have shown that MMI exists as a mixture of monomer and hydrogen-bonded cyclic dimer, even in dilute solution.[3] A particular type of tautomerization of MMI is H_2O-assisted tautomerization, in which H_2O molecules mediate the process by serving as a bridge that connects the donor and acceptor sites. Another type of proton transfer may take place through a self-association machanism. Although tautomerization of thione/thiol has been of interest to chemists for a very long time, the hydrogen-bond interactions between the tautomers of MMI and water, and the information for the water-assisted and self-assisted proton-transfer reactions of thione/thiol tautomerism have not yet been considered. Only one recent paper has reported the direct, H_2O-monomer-assisted and $(H_2O)_2$-assisted proton-transfer reactions in 2-mercaptoimidazole (**C** compound).[8] In this work, density functional theory was used to investigate the proton transfer via intramolecular mechanism, water-assisted and self-assisted tautomerization of MMI and its derivative.

Among weakly bound systems, hydrogen bonding has attracted increasing interest, both theoretically and experimentally, over the past several years, given its relevance in chemical and biological systems and in supramolecular chemistry.[9–11] In several sulfur HB complexes, the interacting hydrogen of the acid gains charge upon complexation, in sharp contrast to the conventional picture of hydrogen bonding.[12] In view of this controversy, characterization of HBs in sulfur-containing complexes is significant to understand the chemical and biological properties of these molecules. Thus, in the second part of this work, the SH···N, S···HN, S···HO, and SH···O H-bonds were characterized by using atoms in molecules (AIM)[13] and natural bond orbital (NBO)[14] analyses.

Computational Details

All calculations were performed using the Gaussian 98 program package.[15] The geometries of the monomers, dimers and transition states for the tautomerization processes were optimized using B3LYP method applying 6-311++G(2d,2p) basis sets. The reliable accurate description of weak interactions like HBs generally requires a treatment of electron correlation. Density functional calculations with Becke three parameter hybrid method using the correlation functional of Lee, Yang, and Parr (B3LYP)[16,17] have proved quite useful in this regard for studying systems with HBs.[18–23] DFT offers an electron correlation correction frequently comparable to the MP2 or in certain cases, and for certain purposes even superior to

Published on the web November 12, 2008; doi:10.1246/bcsj.81.1402

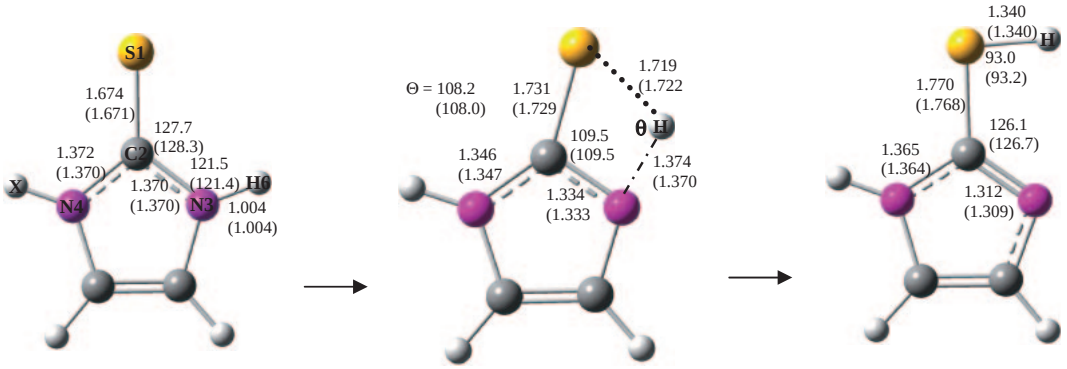

A: X = Me **A-TS** **B: X = Me**
C: X = (H) **C-TS** **D: X = (H)**

Figure 1. Selected optimized geometrical (distances in Å and angles in °) parameters in the direct proton-transfer mechanism **A**(**C**) → **A**(**C**)-TS → **B**(**D**) at B3LYP/6-311++G(2d,2p) level in the gas phase.

MP2, but at considerably lower computational cost.[18] Vibrational frequencies have been obtained at the same level for characterization of stationary points and thermal zero-point energy corrections. To establish the connection between the transition state structures and corresponding equilibrium structures, intrinsic reaction coordinate (IRC) analysis was carried out at B3LYP/6-311++G(2d,2p) level. Natural bond orbital (NBO) analysis was carried out with version 3.1 included in the Gaussian-98 program at B3LYP/6-311++G(2d,2p) level of theory. In addition, topological properties have been calculated using AIM methodology on the wave functions obtained at B3LYP/6-311++G(2d,2p) level by the AIM2000 program package.[24]

Results and Discussion

Geometries. The equilibrium structures and transition state complexes for different paths of proton transfer in MMI at B3LYP/6-311++G(2d,2p) level of theory are shown in Figures 1 and 2. Dimers **AA** and **CC** have two S···HN H-bonds and dimers **BB** and **DD**, which are tautomeric forms of **AA** and **CC** dimers, respectively, have two N···HS H-bonds. Furthermore, structural parameters of **A**(**C**)**W**, **B**(**D**)**W**, **A**(**C**)**2W**, and **B**(**D**)**2W** complexes and corresponding transition states for the H_2O-assisted tautomerization are given in Figure 2. **A**(**C**)**W** and **B**(**D**)**W** complexes are stabilized by two S···H–O and N–H···O, and two S–H···O and N···H–O nonlinear hydrogen bonds, respectively.

During the direct proton-transfer mechanism (**A**(**C**) → TS → **B**(**D**)), the N–C and C–S bond lengths change from 1.370 (1.370 Å) and 1.674 (1.671 Å) to 1.334 (1.333 Å) and 1.731 (1.729 Å), respectively. The N–C–S angle is closed by 18.2 (18.8°) from **A**(**C**) to TS, a 14.0% decrease. The N–H distance is then stretched from 1.004 (1.004 Å) to 1.334 (1.333 Å), an increase of (32%) to reach the TS. Thus, for direct tautomerization to takes place, the **A**(**C**) must undergo large structural changes in which are energetically expensive. Such geometric variations make the direct proton transfer difficult. These structural changes reflect the process of the formation of new S–H bond and an old N–H bond dissociation.

All four dimers **AA**–**DD** have cyclic configuration. In contrast to dimers **BB** and **DD**, both monomers in dimers **AA** and **CC** are in the same plane (Figure 1). Dimers **AA** and **CC** are stabilized by two of the same nonlinear HBs with computed N–H···S angel of 173.9 and 174.6°, respectively. The calculated intermolecular H···S distances for dimers **AA** and **CC** at B3LYP/6-311++G(2d,2p) level of theory are 2.301 and 2.288 Å, respectively. From comparison between N–H and C–S bond lengths in the dimers **AA** and **CC** with their corresponding monomers, it is obvious that dimerization yields an increase of the N–H and C–S distances. Furthermore, due to dimerization the bond lengths of N2–C3 and N4–C3 decrease and bond angles of N3–C2–S1 and H5–N3–C2 increase.

Dimers **BB** and **DD** are stabilized by two nonlinear S···HO and O···HN HBs with bond angles of 180.0 and 179.4°, respectively. The analysis of the geometrical parameters shows that the complexation causes lengthening of the C2–N3 and S–H5 bonds and shortening of the C–S bond. The change of N3–C2–S1 angle is minor. The SH···N distances in **BB** and **DD** complexes are 1.843 and 1.874 Å, respectively.

The geometrical parameters of the dimers and transition states for the tautomeric interconversion within a self-associated process (**AA**(**CC**) → **AA**(**CC**)-TS → **BB**(**DD**)-TS) at B3LYP/6-311++G(2d,2p) level are illustrated in Figure 2. As shown in this figure, NH···S distances decrease and N–H distances increase on going from ground states to TSs. The other structural changes are lengthening of the C–S bonds and shortening of the C–N bonds in GS → TS processes. The results also show that the NH···S bonds are nearly linear hydrogen bonds (174.0°), causing the H atoms to more easily transfer. In comparison with direct tautomerization, the NCS angle in **AA**(**CC**) → **AA**(**CC**)-TS processes is also compressed by only ≈1.0° (≈19.0° in **A**(**C**) → **A**(**C**)-TS).

The structure of **A**-H_2O (**AW**) and **C**-H_2O (**CW**) complexes are given in Figure 2. Dimers **AW** and **CW** are stabilized by two nonlinear S···HO and O···HN HBs with bond angles of 150.9 and 150.1°, respectively. The calculated intermolecular distances of S···HO and O···HN in these complexes are 2.346 (2.354 Å) and 1.923 (1.916 Å), respectively. From Figure 2, it is obvious that dimerization yields to increase of the N–H and C–S bonds. Also, dimerization causes the bond lengths of N2–C3 and N4–C3 to decrease. The bond angles of N3–C2–S1 and H5–N3–C2 in complexes are similar to those of related monomers. Surveying the calculated structural parameters of H_2O reveals that changes in the H_2O geometries upon

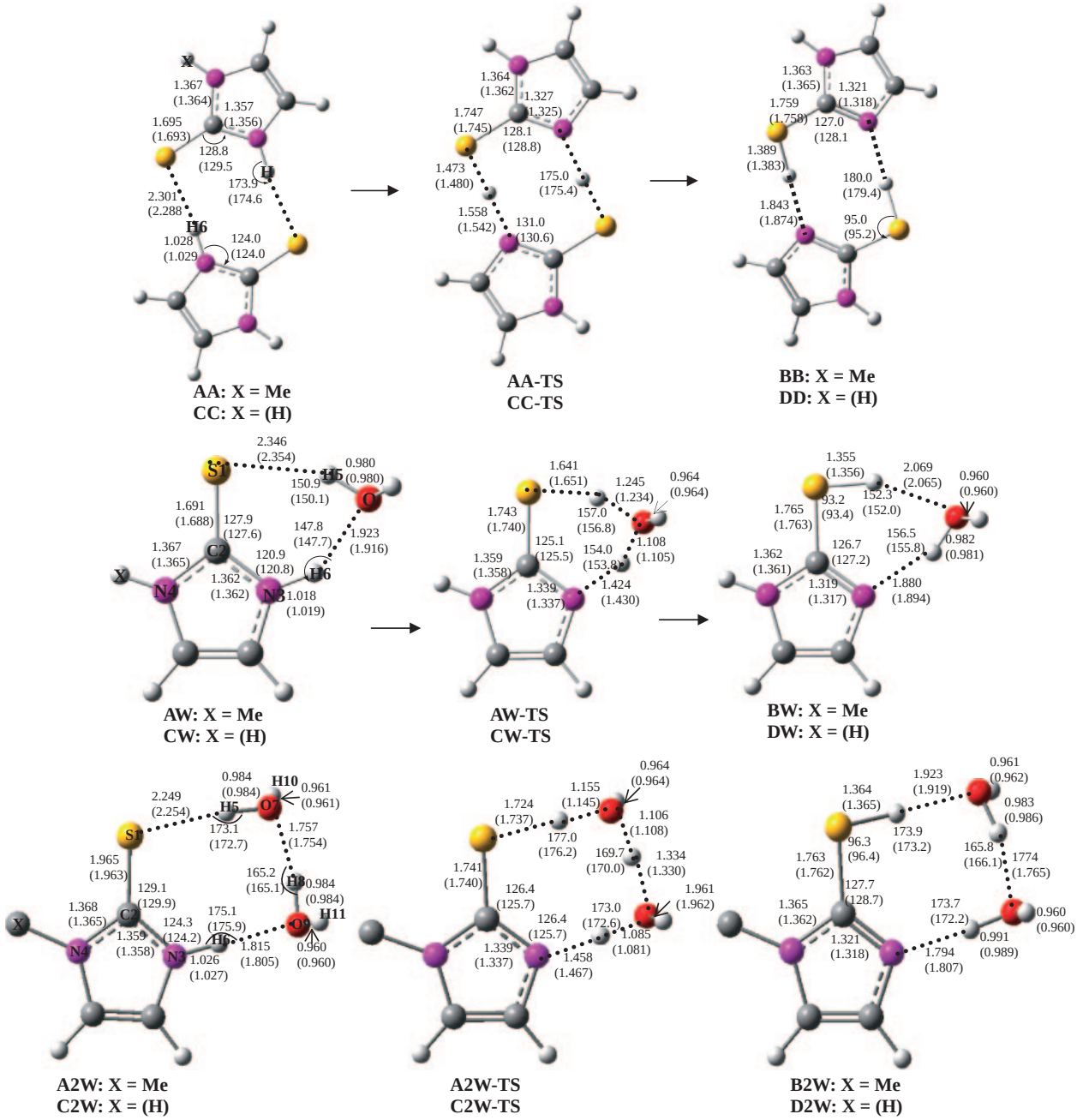

Figure 2. Selected optimized geometrical (distances in Å and angles in °) parameters in the mechanism of proton transfer in self-associated, monohydrated, and dihydrated forms of **MMI** and its derivative at B3LYP/6-311++g(2d,2p) level in the gas phase.

complexation are also minor. Complexation induces a small elongation of the O–H5 bond (0.019 Å) and HOH angle (0.5°).

W-TSs are transition states predicted in H_2O-assisted tautomerization of **A** and **C** monomers. The TS structures constitute a first-order saddle point whose negative force constant is assisted by the asymmetric stretch of water. During the H_2O-assisted hydrogen-transfer reaction (**A**(**C**)**W** → TS → **B**(**D**)**W**), water acts simultaneously as a proton acceptor and donor, which can also be concluded by our NBO analysis. In contrast to **BW** and **DW**, the six-membered ring in **AW** and **CW** is planar with an O–H bond of H_2O stretching out of plane. In both monomers, complexation induces elongation of the C–S bond and reduction of the C–N bond. In both dimers **AW** and **CW**, NH···O and S···HO distances decrease, while N–H_b and O–H_b distances increase on going from ground states to TSs. The computed N–H···O and S···H–O angles in **AW** and **CW** increase on going from ground states to TSs.

The structure of **A2W** to **D2W** complexes are given in Figure 2. In thione complexes **A**(**C**)**2W**, in which dimers of water act simultaneously as the proton donor and proton acceptor, three S···HO, O···HO, and O···HN hydrogen bonds are observed. The computed S···HO, O···HO, and O···HN distances are 2.249 (2.254 Å), 1.757 (1.754 Å), and 1.815 (1.805), which are shorter than those of **A**(**C**)**W**. In addition, the bond lengths of N–H and O–H in these complexes are larger than those of **A**(**C**)**W**. This means that the interactions in

Table 1. Selected Vibrational Frequencies (cm^{-1}) for Monomers and Complexes and Binding Energies ($kJ\,mol^{-1}$) in the Self-Assisted and H_2O-Assisted Proton-Transfer Mechanisms at B3LYP/6-311++G(2d,2p) Level

	ΔE_{elec}	ΔE_0[a)]	ΔE[b)]	ΔH[c)]	ν(S–H)	ν(N–H)	ν(O–H)
AA	−62.3	−59.1	−51.6	−54.1		3252.4 (3677.4)[d)]	
BB	−40.2	−35.5	−29.0	−31.5	2121.5 (2682.4)[d)]		
CC	−64.2	−60.7	−53.4	−55.9		3235.7 (3676.2)[d)]	
DD	−40.0	−34.5	−27.5	−30.0	2179.6 (2685.8)[d)]		
AW	−44.1	−35.0	−25.8	−28.3		3414.6	3498.6 (3925.4)[d)]
BW	−38.1	−28.1	−18.4	−20.9	2509.5		3437.7
CW	−44.4	−35.2	−26.1	−28.6		3408.6	3505.5
DW	−37.2	−26.8	−17.2	−19.7	2508.1		3462.0
A2W	−87.08	−67.95	−49.15	−54.07		3268.1	3453.8
C2W	−87.88	−68.74	−49.98	−54.93	2403.6		3455.1[e)] 3256.7[f)]
B2W	−78.21	−57.89	−38.84	−43.76		3252.1	3454.9
D2W	−77.81	−57.31	−38.13	−43.05	2396.1		3463.0[e)] 3289.0[f)]

a) $E_0 = E_{elec} + ZPE$. b) $E = E_0 + E_{therm}$. c) $H = E_0 + H_{therm}$. d) For monomers. e) For O–H···O. f) For O–H···N.

these complexes are stronger than in **A(C)W**. The change of structural parameters on going from ground state to transition state in **A(C)2W** complexes is greater than those of **A(C)W**.

From comparison of structural parameters in the **A(C)** → **A(C)**-TS process and **AA(CC)** → **AA(CC)**-TS, **A(C)–W** → **A(C)W**-TS and **A(C)–2W** → **A(C)2W**-TS processes, it can be concluded that changes in the framework of the monomer **A(C)** are greater in **A(C)**-TS than those of **AA(CC)**-TS, **A(C)W**-TS and **A(C)2W**-TS. The smaller deformation of structure of monomers **A** and **C** in **AA(CC)** → **AA(CC)**-TS, **A(C)–W** → **A(C)W**-TS and **A(C)–2W** → **A(C)2W**-TS processes causes the H atom easier to transfer more easily in these processes than in **A(C)** → **A(C)**-TS). As a result, the lower energy barrier for **AA(CC)** → **AA(CC)**-TS, **A(C)–W** → **A(C)W**-TS and **A(C)–2W** → **A(C)2W**-TS processes can be attributed to the smaller deformation of structure of monomers **A** and **C** in these processes with respect to **A(C)** → **A(C)**-TS).

Energetics and Frequencies. The electronic binding energies together with thermal and zero-point corrected energies for different dimers of **AA** to **DD** and **AW** to **D2W** at B3LYP/6-311++G(2d,2p) level of theory are given in Table 1. From Table 1, binding energies obtained using 6-311++G(2d,2p) basis set are $-62.3\,kJ\,mol^{-1}$ for dimer **AA**, $-64.2\,kJ\,mol^{-1}$ for dimer **CC**, $-40.2\,kJ\,mol^{-1}$ for dimer **BB**, and $-40.0\,kJ\,mol^{-1}$ for dimer **DD**. The stability of dimers decreases in the order of **CC** > **AA** > **DD** > **BB**. The inclusion of BSSE correction at B3LYP/6-311++G(2d,2p) level of theory has a minor effect on the binding energy, so this correction is not discussed. The energy of a single N–H···S=C HB in dimers **AA(CC)** is 31.15 (32.1) $kJ\,mol^{-1}$ and that of N···HS HB in dimers **BB(DD)** is 20.0 (20.1) $kJ\,mol^{-1}$. These results indicate that the most stable dimers have two N–H···S=C types HBs. As a result, stability of dimers increases with increment of the number of H···S type hydrogen bonds.

To examine the influence of zero-point and thermal energies on binding energy, these energies including ZPE and thermal correction energies are also reported in Table 1. At the B3LYP/6-311++G(2d,2p) level of theory, the ZPE correction ranges from 5.1% in dimer **AA** to 13.8% in dimer **DD**. Contribution of ZPE energy reduces in going from dimers **AA** and **CC** to dimers **BB** and **DD**. The range of thermal correction is 9.4%, **AA**, 16.1%, **BB**, 11.5%, **CC**, and 17.4%, **DD**.

The difference between the two types of hydrogen bonds predicted in dimers **AA(CC)** and **BB(DD)** is also apparent in the vibrational frequency of N–H and S–H bonds. The calculated vibrational frequency shift of N–H and S–H bonds for dimers **AA–DD** as compared to monomers are presented in Table 2. B3LYP/6-311++G(2d,2p) computations predict that the highest vibrational frequencies correspond to the N–H bond of dimers, which are red-shifted from that of the corresponding monomers. The N–H frequency corresponding to the N–H···S=C interaction for dimers **AA** and **CC** is red-shifted by 425.0 and 440.5 cm^{-1} at the B3LYP/6-311++G(2d,2p) level, respectively. The calculated red shift of vibrational frequency of an S–H bond involved in S–H···N=C interaction at B3LYP/6-311++G(2d,2p) level is 560.9 and 506.2 cm^{-1} in dimers **BB** and **DD**, respectively. A comparison between red shift of N–H and S–H vibrational frequencies reveals that the value of red shift in the N–H···S=C type hydrogen bond is smaller than that in S–H···N=C. Vibrational frequency changes for N–H and S–H bonds upon dimerization are completely in agreement with their corresponding bond length changes.

The binding energies for **AW** to **D2W** are given in Table 1. ZPE and thermal corrections influence the binding energies.

Table 2. Calculated Activation Energies (kJ mol^{-1}) for the Direct, Self-Assisted, and H_2O-Assisted Proton-Transfer Mechanisms at B3LYP/6-311++G(2d,2p) Level

	$\Delta^{\#}E_{elec}$	$\Delta^{\#}E_0$[a)]	$\Delta^{\#}E$[b)]	$\Delta^{\#}H$[c)]	$\Delta^{\#}G$[d)]
A → **A**-TS	174.4	157.2	137.4	137.4	143.3
C → **C**-TS	172.7	155.9	138.6	138.6	139.4
AA → **AA**-TS	117.1	89.6	57.9	57.9	74.0
CC → **CC**-TS	112.2	84.0	51.7	51.7	69.0
AW → **AW**-TS	86.6	68.5	44.6	44.6	58.8
CW → **CW**-TS	84.4	66.9	45.8	45.8	54.1
A2W → **A2W**-TS	88.0	68.2	43.5	43.5	54.8
C2W → **C2W**-TS	84.8	65.8	41.7	41.7	53.0

a) $E_0 = E_{elec} + ZPE$. b) $E = E_0 + E_{therm}$. c) $H = E_0 + H_{therm}$. d) $G = E_0 + G_{therm}$.

As can be seen in Table 1, binding energy of dimers **AW** to **DW** is smaller than corresponding dimers **AA** to **DD**. Thus, hydrogen-bond interaction in the self-association complexes is stronger than water-associated complexes. In addition, inclusion of a water molecule to **A**(**C**)**W** complexes increases the binding energy and therefore their stability by about 43.0 (43.5 kJ mol^{-1}).

Binding energies of **B**(**D**)**W** and **B**(**D**)**2W** species are smaller than those of **A**(**C**)**W** and **A**(**C**)**2W**, respectively. Thus, effect of hydration is to favor the stability of the thione forms over than the thiols. Similar to the case of self-associated complexes, inclusion of BSSE correction at B3LYP/6-311++G(2d,2p) level of theory has minor effect on the binding energy, so this correction is not discussed. At the B3LYP/6-311++G(2d,2p) level of theory, the sum of the contributions of ZPE and thermal energy have major effect on the magnitude of binding energies.

From Table 2, B3LYP/6-311++G(2d,2p) computations predict that the highest vibrational frequency in water-assisted complexes correspond to the O–H bond of water, which are red-shifted from that of isolated water. The O–H frequency that corresponds to the O–H···S=C interaction for dimers **AW** and **CW** is red-shifted by 426.8 and 419.9 cm^{-1} at B3LYP/6-311++G(2d,2p) level, respectively. The calculated red shift of vibrational frequency of the O–H bond involved in O–H···N=C interaction at the B3LYP/6-311++G(2d,2p) level is 487.7 and 463.4 cm^{-1} in dimers **BW** and **DW**, respectively. The calculated red-shift of vibrational frequency of the N–H bond in dimers **AW** and **CW** is 262.8 and 268.8 cm^{-1}, respectively. In comparison with **B** and **D**, vibrational frequency of the S–H bond involved in S–H···O interaction in dimers **BW** and **DW** is also red-shifted by 172.9 and 176.3 cm^{-1}, respectively. A comparison between red shift of O–H, N–H, and S–H vibrational frequencies reveals that the value of red shift in the O–H···S=C type hydrogen bond is greater than others. Vibrational frequency changes for O–H, N–H, and S–H bonds upon dimerization are completely in agreement with their corresponding bond length changes. Compared to **W**-assisted complexes, red shift of O–H and N–H vibrational frequencies in formation of **2W**-assisted complexes is greater, in agreement with change in these bond distances upon complexation.

Barrier Energy. The energy barriers including ZPE corrections for four proton-transfer reactions at B3LYP/6-311++G(2d,2p) level are listed in Table 3. We also present a profile of potential energy changes for these proton-transfer

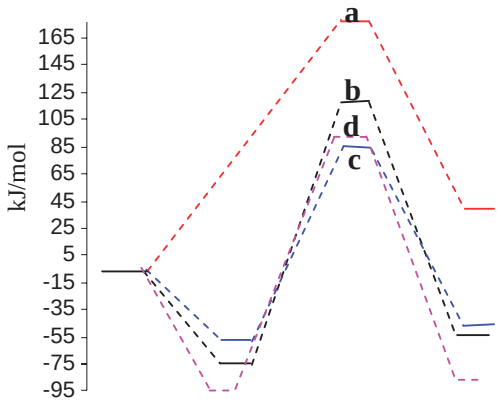

Figure 3. Relative potential energy profile for proton transfer reactions in **A** (**MMI**): (a) **A** → **A**-TS → **B**, (b) **AA** → **AA**-TS → **BB**, (c) **AW** → **AW**-TS → **BW**, and (d) **A2W** → **A2W**-TS → **B2W**.

mechanisms in Figure 3. As can be seen from Table 3, inclusion of zero-point and thermal energies decreases the barrier height. The activation Gibbs energies for (**A**(**C**) → **A**(**C**)-TS), (**AA**(**CC**) → **AA**(**CC**)-TS), (**A**(**C**)**W** → **A**(**C**)**W**-TS), and (**A**(**C**)**2W** → **A**(**C**)**2W**-TS) proton transfers are 143.3 (139.4), 74.0 (69.0), 58.8 (54.1), and 43.5 (41.7) kJ mol^{-1}, respectively. Consequently, barrier heights for both self-assisted and H_2O-assisted proton transfers are significantly lower than that of the direct proton transfer. Thus, tautomerization is facilitated by self-association and inclusion of H_2O. The energy barrier for self-assisted proton transfer is greater than H_2O-assisted transfer. As a result, H_2O-assisted tautomerization is energetically a suitable path for proton transfer. With respect to H_2O-monomer-assisted, the second water molecule in the bridging site of **A**(**C**)**2W** reduces activation Gibbs free energy by 4.0 (1.1 kJ mol^{-1}). The calculated activation Gibbs energies for compound **C** are in agreement with the results obtained by Zhu et al.[8] at the B3LYP/6-311+G(d,p) level for direct (56.8 kJ mol^{-1}), H_2O-monomer-assisted (69.3 kJ mol^{-1}), and $(H_2O)_2$-assisted (66.5 kJ mol^{-1}) proton-transfer reactions.

Compared with **A**(**C**) → **B**(**D**), decrease in the reaction energies for self-assisted and H_2O-assisted proton transfers are greater (Table 1), and activation energies are also lower (Table 2). Thus, it can be concluded that the direct proton transfer is more difficult than the water-assisted and self-assisted processes both thermodynamically and dynamically.

Table 3. Bond Critical Point Properties (au) of Monomers and Dimers at B3LYP/6-311++G(2d,2p) Level of Theory

	$\rho(r)$	$\nabla^2\rho(r)$	$H(r)$	$\rho(r)$	$\nabla^2\rho(r)$	$H(r)$	$\rho(r)$	$\nabla^2\rho(r)$	$H(r)$
	A(C)			**B(D)**			**A(C)**-TS		
S1–C2	0.2088	−0.3009	−0.2142	0.1891	−0.2716	−0.2129	0.1955	−0.2837	−0.1517
	0.2095[a)]	−0.2922	−0.2186	0.1901	−0.2764	−0.1248	0.1956	−0.285	−0.1538
C2–N3	0.3174	−0.9834	−0.4251	0.3705	−1.1771	−0.5052	0.3567	−1.1578	−0.4857
	0.3178	−0.9871	−0.4243	0.3728	−1.188	−0.5115	0.358	−1.1654	−0.4887
N3–H6	0.3516	−1.9255	−0.5329				0.1239	−0.0869	−0.0768
	0.3515	−1.9276	−0.5332				0.1251	−0.093	−0.0784
S1–H5				0.2153	−0.5964	−0.1981	0.0944	−0.0533	−0.043
				0.2155	−0.5958	−0.1979	0.0938	−0.0513	−0.0424
	AA(CC)			**BB(DD)**			**AA(CC)**-TS		
S1–C2	0.2053	−0.3155	−0.1900	0.1915	−0.2847	−0.1324	0.1938	−0.2919	0.1938
	0.2038[a)]	−0.314	−0.1933	0.1913	−0.2822	−0.1314	0.1941	−0.2949	0.1941
C2–N3	0.3278	−1.0322	−0.4451	0.6347	−1.1631	0.4984	0.356	−1.1284	0.3560
	0.3291	−1.0404	−0.4472	0.3622	−1.1497	−0.4908	0.3577	−1.1390	0.3577
S1–H5	0.0253	0.0447	−0.0018	0.2008	−0.5162	−0.1642	0.0801	0.0483	0.0801
	0.0259	0.045	−0.0020	0.1987	−0.5064	−0.161	0.0834	0.0417	0.0834
N3–H5	0.3280	−1.864	−0.5139	0.0378	0.0808	−0.0022	0.1646	−0.3436	0.1646
	0.3269	−1.8577	−0.5222	0.0406	0.0822	−0.0033	0.1617	−0.3302	0.1617
	A(C)W			**B(D)W**			**A(C)W**-TS		
S1–C2	0.2045	−0.3123	−0.1953	0.1901	−0.185	−0.2764	0.1927	−0.281	−0.1445
	0.2051[a)]	−0.3093	−0.1999	0.1908	−0.1875	−0.2806	0.1931	−0.2842	−0.1472
C2–N3	0.3245	−1.0158	−0.4353	0.3642	−0.6936	−1.1503	0.3485	−1.0864	−0.4578
	0.3255	−1.0221	−0.4362	0.3664	−0.7034	−1.1626	0.3501	−1.0956	−0.4617
N3–H6	0.3376	−1.9484	−0.5344	0.2122	−0.025	0.0876	0.1078	−0.0085	−0.0574
	0.337	−1.9492	−0.5344	0.2120	−0.0239	0.0864	0.1060	−0.0027	−0.0554
O–H5	0.3494	−2.5679	−0.7152	0.3462	−0.0139	0.067	0.1618	−0.2477	−0.1395
	0.3498	−2.5729	−0.7163	0.3476	−0.0141	0.0676	0.1665	−0.2866	−0.1500
O–H6	0.0273	0.0913	0.0011	0.0343	−0.7858	−2.5607	0.2340	−1.1268	−0.3667
	0.0277	0.0924	0.001	0.0332	−0.7891	−2.5742	0.2360	−1.1602	−0.3745
S1–H5	0.0231	0.0445	−0.0013	0.0216	−0.2265	−0.5787	0.1115	−0.1295	−0.0611
	0.0226	0.0442	−0.0012	0.0218	−2.2603	−0.5772	0.1088	−0.1199	−0.0586
	A(C)2W			**B(D)2W**			**A(C)2W**-TS		
C2–S1	0.2035	−0.3149	−0.1902	0.1928	−0.3070	−0.1380	0.1930	−0.2847	−0.1454
	0.2040[a)]	−0.3135	−0.1944	0.1931	−0.3100	−0.1398	0.1933	−0.2874	−0.1476
S1–H5	0.0272	0.0464	−0.0026	0.2046	−0.4683	−0.1557	0.0915	−0.0667	−0.0440
	0.0269	0.0462	−0.0025	0.2039	−0.4646	−0.1548	0.0886	−0.0581	−0.0417
O7–H5	0.3439	−2.5260	−0.7044	0.0309	0.0809	−0.0009	0.2051	−0.7077	−0.2588
	0.3444	−2.5311	−0.7056	0.0313	0.0820	−0.0009	0.2107	−0.7807	−0.2770
O7–H10	0.3730	−2.6983	−0.7536	0.3728	−2.2584	−0.6439	0.3687	−2.7167	−0.7529
	0.3730	−2.7009	−0.7541	0.3729	−2.2584	−0.6439	0.3685	−2.7199	−0.7534
O7–H8	0.0388	0.1133	−0.0017	0.3417	−2.1057	−0.5990	0.2326	−1.1422	−0.3714
	0.0389	0.1137	−0.0018	0.3423	−2.1085	−0.5997	0.2309	−1.1186	−0.3656
O9–H8	0.3434	−2.5537	−0.7099	0.0395	0.1130	−0.0016	0.1202	0.0200	−0.0710
	0.3431	−2.5528	−0.7095	0.0390	0.1115	−0.0016	0.1214	0.0138	−0.0730
O9–H11	0.3734	−2.6961	−0.7537	0.3730	−2.2563	−0.6437	0.3714	−2.6837	−0.7501
	0.3733	−2.6970	−0.7538	0.3728	−2.2584	−0.6440	0.3713	−2.6875	−0.7506
O9–H6	0.0346	0.1017	−0.0009	0.3310	−1.9967	−0.5729	0.2487	−1.3495	−0.4215
	0.0354	0.1033	−0.0011	0.3330	−2.0155	−0.5775	0.2518	−1.3985	−0.4331
N3–H6	0.3300	−1.9191	−0.5266	0.0441	0.1004	−0.0036	0.0989	0.0187	−0.0475
	0.3290	−1.9171	−0.5259	0.3330	−2.0155	−0.5775	0.0966	0.0251	−0.0451
N3–C2	0.3265	−1.0246	−0.4396	0.3639	−1.3030	−0.5368	0.3473	−1.0855	−0.4580
	0.3277	−1.0321	−0.4413	0.3661	−1.3241	−0.5493	0.3490	−1.0957	−0.4625

a) For species given in parenthesis.

Most energy saving is achieved in assisted tautomerization because structural parameters need not be changed to such a large extent as the direct proton transfers. The large reduction in the energy barriers of water and self-assisted tautomerizations with respect to direct tautomerization can be attributed to smaller deformation of structures in these processes. Hence, water and self-assisted tautomerizations are more energetically and structurally favored and proton transfer occurs more easily.

Atoms in Molecules (AIM) Analysis. The quantum theory of atoms in molecules (QTAIM) is a useful tool to characterize hydrogen bonding.[25–29] The calculated values of electron density, $\rho(r)$, Laplacian of electron density, $\nabla^2\rho(r)$, and electronic energy density, $H(r)$, at the bond critical points (BCPs) at B3LYP/6-311++G(2d,2p) level of theory are listed in Table 3. Besides the local topological properties at the bond critical points, a set of atomic integrated properties such as atomic charge $q(\Omega)$, atomic energy $E(\Omega)$, and atomic volume $V(\Omega)$ can be calculated by topological analysis. These values are reported in Table 4. The molecular graphs (including the critical points and bond paths) of the all complexes are shown in Figure 4.

The comparison between BCP data of the N–H bond in ground ($\rho(r) = 0.3516$, $\nabla^2\rho(r) = -1.9255$, and $H(r) = -0.5329$ au) and transition states ($\rho(r) = 0.1239$, $\nabla^2\rho(r) = -0.0869$, and $H(r) = -0.0768$ au) of **A**(**C**) shows that the covalent nature of this bond decreases on going from ground state to transition state. Besides N–H BCP, one additional BCP is also observed in the S···H distance of transition state. The partially covalent nature of S···H distance in the transition state can be concluded from the electron density properties of $\nabla^2\rho(r)$ and $H(r)$.

Besides all of the expected BCPs, the electron density reveals two additional BCPs in H···S distances of the **AA** and **CC** complexes. This interaction generates a cyclic system with a ring critical point (RCP) (Figure 4). The electron density of the critical point of a weak interaction is twenty times less than the electron density of a normal interaction. In **AA**(**CC**) complexes, values of $\rho(r)$, $\nabla^2\rho(r)$, and $H(r)$ at H···S BCP are 0.0253 (0.0259 au), 0.0447 (0.0450 au), and −0.0018 (−0.0020 au), respectively. The values of the $\rho(r)$ and $\nabla^2\rho(r)$ at H···S critical point are in the typical range of (0.002–0.035 au) and (0.020–0.139 au) for H-bonding, respectively. The small electron density and positive values of $\nabla^2\rho(r)$ at S···HN BCP are typical for closed-shell interactions or electrostatic character of the hydrogen bonding. However, small negative value of $H(r)$ reveals some contribution of sharing interaction (partially covalent) to the S···HN bond. The values of $\rho(r)$, $\nabla^2\rho(r)$, and $H(r)$ at the BCP of N–H bond in **AA** and **CC** predict that N–H bonds have covalent character. Comparison of the $\nabla^2\rho(r)$ and $H(r)$ at the N–H BCPs of **AA** and **CC** complexes with corresponding values of monomers, show that the participation of the N–H bond in HBs causes lowering of the negative $\nabla^2\rho(r)$ and $H(r)$ values and hence lowering of the covalent contribution to N–H bond. The values of $\rho(r)$, $\nabla^2\rho(r)$, and $H(r)$ at the BCP of S···H contact of **AA** and **CC** increase and that of N···H contact decrease on going from ground state to transition state. These values in **AA**-TS and **CC**-TS reveal the covalent nature of the S···H bond and partially covalent nature of N···H bond.

The calculated $\rho(r)$, $\nabla^2\rho(r)$, and $H(r)$ values for the N···H bonding in **BB** (0.0378, 0.0808, and −0.0022 au, respectively) and **DD** (0.0406, 0.0822, and −0.0033 au, respectively) complexes indicate that the SH···N bonds are partially covalent in nature. Furthermore, comparison of the $\nabla^2\rho(r)$ and $H(r)$ values in S–H bond of **BB** and **DD** complexes with the corresponding monomers reveal that the covalent nature of S–H bonds in **B** and **D** decrease upon complexation.

As can be seen in Table 3, electron density at the N–H6 and O–H5 BCPs of monomers **A**(**C**) and **W** decreases upon complexation, in agreement with the increase of the corresponding bond distances. Negative values of $\nabla^2\rho(r)$ and $H(r)$ at N–H6 covalent bond of **A**(**C**) monomers increase and those of O–H5 decrease, indicating the covalent nature of N–H6 bond increases and that of O–H5 decreases upon complexation.

The calculated electron density properties of **A**(**C**)**W** show that both S···H5 and O···H6 HBs have low $\rho(r)$ and positive $\nabla^2\rho(r)$. Additionally, $H(r)$ values for the S···H5 and O···H6 HBs are negative and positive, respectively. These values reveal the partially covalent nature of S···H5 interaction and electrostatic nature of O···H6 interaction. For **A**(**C**)**W** → **A**(**C**)**W**-TS → **B**(**D**)**W** processes, comparison of electron density properties of N–H6 and O–H5 bonds reveals that the $\rho(r)$, $\nabla^2\rho(r)$, and $H(r)$ values of both bonds decrease upon hydrogen transfer. On the other hand, $\rho(r)$, $\nabla^2\rho(r)$, and $H(r)$ values for S···H5 and O···H6 HBs increase in agreement with change of bond distances observed upon hydrogen-transfer mechanism. This indicates that the HBs for transition states are stronger than ground states.

In **A**(**C**)**2W** complex, for all covalent bonds involved in hydrogen bonds, i.e. for N–H in N–H···O9, O9–H in O9–H···O7, and O7–H in O7–H···S, electron densities at the corresponding BCPs are high and the Laplacian of the electron densities as well as $H(r)$ values are negative, indicating the covalent character of these bonds. Analysis of BCP data reveals that the covalent nature of these interactions decreases upon **A**(**C**)**W** → **A**(**C**)**W**-TS process. The $H(r)$ values for the NH···O9 and O9H···O7 HBs are negative, suggesting the electrostatic nature of these interactions. The negative $H(r)$ values for NH···O9 and O9H···O7 HBs increase on going from ground state to transition state. This indicates that the HBs for transition states are stronger than ground states. The O7H···S HB has partially covalent nature and it increases slightly on going from ground state to transition state.

From Table 4, comparison of integrated properties for the **A**(**C**) and **A**(**C**)-TS shows that electronic population (as a measure of atomic charge) of H atom involved in S–H···N interaction increases in going from **A**(**C**) to **A**(**C**)-TS. In spite of the increase of electron population, atomic volume, and atomic energy increase in this process.

As can be seen in Table 4, electronic populations of S atoms involved in S···HN interactions in **AA** and **CC** complexes increase upon complexation. As a consequence of the gain of electronic charge, the S atoms are stabilized ($\Delta E < 0$) upon dimerization. The values of q_S and q_N correlate well with strength of lp(S) → BD*(N–H) donor acceptor interaction in which are given in the NBO section. The H atoms involved in S···HN interactions lose charge upon interaction. As a result of the loss of electronic charge, H atoms are unstabilized

Table 4. Integrated Atomic Properties (au) of Complexes at B3LYP/6-311++G(2d,2p) Level

Atom	q	E	V	q	E	V	q	E	V
	A(C)			**AA(CC)**			**A(C)**-TS		
S	−0.1437	−398.599	259.1490	−0.2239	−398.664	246.4332	−0.1706	−398.65	239.6086
	−0.1305[a)]	−398.556	261.6440	−0.2050	−398.56	248.3625	−0.1563	−398.618	237.8594
C2	0.5543	−37.6474	58.3857	0.6444	−37.5836	57.1026	0.6769	−37.6691	55.5559
	0.5529	−37.6312	59.2112	0.6170	−37.5984	57.8085	0.6781	−37.6485	56.6798
N3	−0.9788	−55.2583	94.7567	−0.9602	−55.2471	95.1591	−0.9753	−55.1999	105.0412
	−0.9739	−55.2365	94.6840	−1.0269	−55.2848	95.9545	−0.9713	−55.1872	104.4587
H6	0.4174	−0.4588	29.9591	0.4561	−0.4219	22.8485	0.3629	−0.3898	30.5055
	0.4189	−0.4583	29.8187	0.4582	−0.4205	22.6679	0.3644	−0.3896	30.4595
	B(D)			**BB(DD)**			**AA(CC)**-TS		
S	0.1808	−398.58	203.5460	0.0314	−398.672	210.1027	−0.0921	−398.715	217.8965
	0.1821[a)]	−398.555	205.3040	0.0546	−398.565	212.126	−0.0799	−398.607	220.1002
C2	0.7127	−37.6166	55.0869	0.7224	−37.5848	55.3197	0.7103	−37.5863	55.3644
	0.7094	−37.6153	55.4166	0.7261	−37.5866	55.4463	0.7168	−37.5819	55.4628
N3	−0.9181	−55.091	122.3320	−0.9634	−55.1339	107.2239	−0.9204	−55.1251	100.8096
	−0.9064	−55.0638	121.8920	−0.9153	−55.0905	107.3617	−0.9223	−55.1237	100.2410
H6	−0.0175	−0.6058	49.4896	0.1590	−0.5204	32.5417	0.2906	−0.45184	25.1183
	−0.0192	−0.6060	49.5114	0.1538	−0.5238	33.2390	0.2978	−0.4477	24.7089
	A(C)W			**B(D)W**			**A(C)W**-TS		
S	−0.1979	−398.692	246.8290	0.1165	−398.664	205.9754	−0.2231	−398.732	230.4706
	−0.1792[a)]	−398.616	249.6920	0.1329	−398.591	207.0836	−0.2164	−398.661	232.7120
C2	0.5747	−37.6457	57.5288	0.6932	−37.6261	55.262	0.6492	−37.6373	55.6119
	0.5987	−37.6158	57.8192	0.7161	−37.6001	55.2594	0.6638	−37.6153	55.8299
N3	−1.0218	−55.2888	94.3374	−0.9416	−55.1105	109.192	−0.9936	−55.1770	101.9894
	−0.9938	−55.2618	94.0064	−0.9405	−55.1065	109.1229	−0.9937	−55.1722	102.1225
H5	0.5828	−0.3540	18.6029	0.0724	−0.5674	38.2917	0.4321	−0.39099	19.1399
	0.5733	−0.3606	19.0011	0.0760	−0.5656	38.1703	0.4386	−0.3881	18.9525
	(0.5495)[b)]	(−0.3921)	(23.7417)						
H6	0.4773	−0.4267	20.2716	0.6035	−0.3498	14.8701	0.6058	−0.33111	11.9325
	0.4781	−0.4257	20.2228	0.6023	−0.3509	15.0839	0.6071	−0.3305	11.9561
O	−1.135	−75.6568	141.349	−1.1391	−75.6524	142.928	−1.0994	−75.7002	126.1766
	−1.1403	−75.6546	141.304	−1.1435	−75.6558	143.1838	−1.0971	−75.6987	125.6767
	(−1.0933)[b)]	(−75.6706)	(149.418)						
	A(C)2W			**B(D)2W**			**A(C)2W**-TS		
S	−0.1974	−398.7001	244.2555	0.0883	−399.0851	208.5850	−0.2757	−398.7515	233.6474
	−0.2024[a)]	−398.6376	248.7263	0.0822	−399.0484	212.2124	−0.2831	−398.7263	238.5034
C2	0.6065	−37.6380	57.5832	0.7613	−37.4893	55.3740	0.6567	−37.6267	56.5336
	0.6226	−37.6069	57.8362	0.7825	−37.4659	55.4369	0.6724	−37.5971	56.6135
N3	−0.9959	−55.2948	95.1964	−0.9523	−55.1151	107.2016	−0.9875	−55.1646	101.8181
	−0.9890	−55.2529	95.5324	−0.9418	−55.0979	107.3590	−0.9799	−55.1551	101.9781
H5	0.5777	−0.3567	17.1877	0.1303	−0.5404	34.9059	0.4964	−0.3647	16.4392
	0.5799	−0.3555	17.2110	0.1297	−0.5401	34.8285	0.5025	−0.3624	16.2532
H6	0.4957	−0.4146	18.2575	0.6219	−0.3301	13.5309	0.6122	−0.3290	11.1987
	0.4949	−0.4153	18.1728	0.6209	−0.3313	13.6910	0.6144	−0.3278	11.1887
O7	−1.1300	−75.6528	139.5752	−1.1931	−75.6473	142.9690	−1.1034	−75.7267	125.0778
	−1.1306	−75.6495	139.7952	−1.1955	−75.6238	143.2877	−1.1125	−75.7358	125.1781
H10	0.5505	−0.3913	23.7180	0.5697	−0.3736	22.8867	0.5769	−0.3744	22.2296
	0.5532	−0.3899	23.4857	0.5691	−0.3741	22.6834	0.5717	−0.3782	22.4653
H8	0.6247	−0.3413	12.8748	0.6296	−0.3331	13.0343	0.6395	−0.3204	9.7012
	0.6173	−0.3471	13.1207	0.6281	−0.3345	13.1400	0.6399	−0.3201	9.6947
O9	−1.1436	−75.6515	139.9339	−1.2023	−75.6465	141.4169	−1.1522	−75.6999	130.0676
	−1.1563	−75.6691	139.9694	−1.2055	−75.6397	141.6705	−1.1627	−75.7133	130.0664
H11	0.5495	−0.3918	23.6116	0.5703	−0.3726	22.8328	0.5563	−0.3865	23.7281
	0.5517	−0.3906	23.8449	0.5712	−0.3722	22.6944	0.5559	−0.3875	23.5501

a) For species given in parenthesis. b) For H_2O.

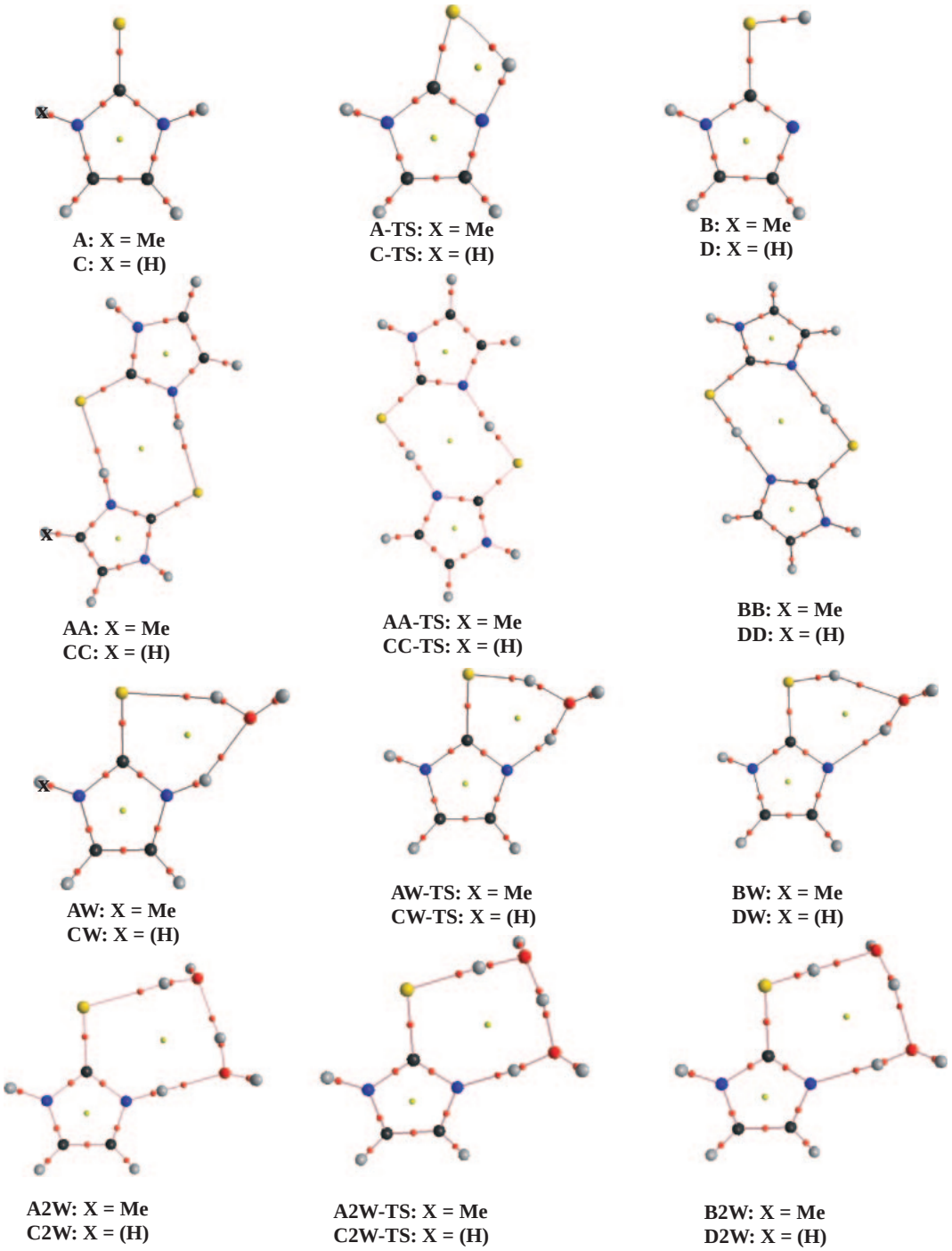

Figure 4. Molecular graphs of compounds. Nuclei and critical points (bond and ring) are represented by big and small circles, respectively.

($\Delta E > 0$) and volume of H atoms decreases. In accord with Koch and Popelier criteria for H-bonding interaction,[28,29] both the electronic population and atomic volume of hydrogen atoms involved in N–H···S interactions decrease and their energies increase upon interaction.

For the **AA**(**CC**) → **AA**(**CC**)-TS processes, electronic charges of bridging protons increase by 0.1655 (0.1604e) and those of N3 decrease by 0.0398 (0.1046e), leading to increase of polarization of the N3–H bond. Furthermore, S atoms lose electronic charge by 0.1318 (0.1251e).

Upon interaction between **A**(**C**) and **W**, H atoms involved in S···H5O and NH6···O interactions lose electronic charge. As a result of the loss of electronic charge, the H atoms are unstabilized ($\Delta E > 0$) and volume of H atoms decreases. Loss of electronic charge, decrease of atomic volume and increase of atomic energy for interacting hydrogen atoms upon both interactions are specific characteristics of conventional HBs.

For the H_2O-assisted processes, electronic charge of H5 in the S···H5O interaction increases and that of H6 and H8 atoms involved in the NH6···O and O9H8···O7 interactions decrease,

Table 5. NBO Data of the Monomers, Complexes, and Transition States at B3LYP/6-311++G(2d,2p) Level

	A(C)	**B(D)**	**AA(CC)**	**BB(DD)**	**A(C)**-TS	**AA(CC)**-TS
Natural charge						
S	−0.2744	0.0304	−0.3259	−0.0349	−0.1602	−0.4235
	−0.2644[a)]	0.0365	−0.3174	−0.0244	−0.1521	−0.0760
C2	0.2441	0.2920	0.2705	0.2708	0.2600	0.2826
	0.2312	0.2270	0.2595	0.2483	0.2453	0.2670
N3	−0.5643	−0.554	−0.5775	−0.5875	−0.6217	−0.5952
	−0.5661	−0.5354	−0.5804	−0.5764	−0.6223	−0.5890
H6	0.4204	0.1587	0.4424	0.2161	0.3409	0.2379
	0.4214	0.1573	0.4429	0.2099	0.3420	0.2390
Occupancy						
σ^*(N–H)	0.0153		0.0770			
	0.0149[a)]		0.0779			
σ^*(S–H)		0.0049		0.0772	0.2622	0.1596
		0.0042		0.0711	0.2633	0.1664
$E^{(2)}$ ($\sigma \rightarrow \sigma^*$)/kJ mol^{-1}						
lp(N3) → σ^*(C–S)	274.2	4.1	<2.0	3.7	4.1	3.0
	277.1[a)]	4.4	<2.0	4.2	4.4	3.5
lp(S) → σ^*(C2–N3)	67.8	106.5	368.3	120.8	153.1	154.5
	70.2	109.7	345.7	117.0	157.1	160.1
lp(S) → σ^*(N–H)			83.6			
			83.6			
lp(N) → σ^*(S–H)				96.8	421.3	259.4
				87.4	428.9	276.3

a) For species given in parenthesis.

respectively. As a consequence of change of electronic density of H atoms, H5 is stabilized and H6 and H8 atoms are destabilized upon tautomerization. In these processes, S atoms gain and O atoms lose electronic charge.

Natural Bond Orbital Analysis. The formation of a hydrogen bond implies that a certain amount of electronic charge is transferred from the proton acceptor to the proton donor molecule.[25] For several typical H-bonded systems, Reed et al.[14] by NBO analysis have demonstrated that the charge is transferred from the lone pairs of the proton acceptors to the antibonding orbitals of the proton donor. The results of NBO analysis including charge-transfer energy, natural charge and the occupancy of NBOs in the monomers and in their complexes at B3LYP/6-31++G(2d,2p) level of theory are given in Tables 5 and 6. From Table 5, electronic charge of S atoms involved in H-bonding in **A(C)** → **A(C)**-TS → **B(D)** processes decreases from −0.2744 (−0.2644e) to −0.1602 (−0.1521e) and then 0.0304 (0.0365e). In contrast, the electronic charge of H atoms involved in H-bonding in these processes increases. Electronic charges of N2 atoms first increase on going from **A(C)** → **A(C)**-TS and then decrease in **B(D)** upon proton-transfer reaction.

The NBO results given in Table 5 show that the specific lp(N) → σ^*(C–S) donor acceptor interaction is a most important interaction in **A(C)** compounds. This interaction disappeared in **AA(CC)** dimers. In addition, interaction energy of lp(S) → σ^*(C2–N3) increases upon dimerization. The charge-transfer energy associated with this interaction is 67.8 (70.2 kJ mol^{-1}) in **A(C)** which increases to 368.3 (345.7 kJ mol^{-1}) in **AA(CC)** dimers and then decreases to 154.5 (160.1 kJ mol^{-1}) in **AA(CC)**-TS. In **AA(CC)** dimers, the charge-transfer energy $E^{(2)}$ corresponding to the lp(S) → σ^*(N–H) intermolecular interactions is 83.6 (83.6 kJ mol^{-1}). The NBO analysis shows that the delocalization energy of lp(N) → σ^*(S–H) interaction in **AA(CC)**-TS is 259.4 (276.3 kJ mol^{-1}).

From Table 5, electronic charge of S atoms involved in H-bonds increases and that of C atoms decreases upon self-association of **A(C)** in agreement with the AIM predictions. Thus, as in numerous HBs, complex formation results in an increase of the polarity of the CS group, the C2 atom loses and the S atom gains electron density. This is as expected from the increase of the C=S distance and decrease of electronic density of C–S BCP which has been discussed in the AIM section. A common feature of both **AA(CC)** dimers is the decrease of the electronic charge on the bridging protons involved in the two NH···S H-bonds. Furthermore, in **AA(CC)** dimers, electronic charge of N atoms in NH···S interaction increases under complex formation. This leads to an increase in N^-H^+ polarity similar to the conventional HBs. From these data, both H and N atoms involved in NH···S HBs gain electronic charge on going from **AA(CC)** to **AA(CC)**-TS. In the present dimers, our results show that there is an increase in the σ^* population of the N–H bonds upon dimerization. During the formation of the dimers, an increase of electronic density in the antibonding orbital of N–H bonds leads to a bond elongation and a red shift of the respective stretching vibration.

From Table 6, it is obvious that specific lp(N) → σ^*(C–S) donor acceptor interaction decreases in **AW(CW)** dimers. The

Table 6. NBO Data of the Complexes and Transition States at B3LYP/6-311++G(2d,2p) Level

	AW (**CW**)	**BW** (**DW**)	**AW** (**CW**)-TS	**A2W** (**C2W**)	**B2W** (**D2W**)	**A2W** (**C2W**)-TS
Natural charge						
S	−0.3189	0.0113	−0.1952	−0.3320	0.0024	−0.2652
	−0.3098[a)]	0.0157	−0.1962	−0.3243	0.0050	−0.2700
C2	0.2620	0.2619	0.2746	0.2649	0.2351	0.2755
	0.2490	0.2468	0.2600	0.2531	0.2129	0.2619
O7	−0.9708	−0.9638	−0.9109	−0.97669	−1.0145	−0.8936
	−0.9702	−0.9622	−0.9072	−0.97650	−1.0124	−0.8923
	(−0.9200)[b)]					
N3	−0.5672	−0.5974	−0.6308	−0.5642	−0.5764	−0.6299
	−0.5691	−0.5931	−0.6317	−0.5662	−0.5696	−0.6302
H6	0.4549	0.4985	0.4949	0.4586	0.5163	0.4908
	0.4562	0.4983	0.4963	0.4594	0.5165	0.4920
	(0.4600)[b)]					
H5	0.4860	0.1930	0.3311	0.4871	0.2042	0.3734
	0.4860	0.1924	0.3356	0.4868	0.2026	0.3784
H8				0.5058	0.5204	0.5042
				0.5063	0.5199	0.5042
O9				−0.9722	−1.0266	−0.9566
				−0.9719	−1.0260	−0.9532
Occupancy						
σ^*(N3–H)	0.0368			0.0506		
	0.0371[a)]			0.0518		
σ^*(O7–H5)	0.0400			0.0547		
	0.0390			0.0540		
σ^*(O7–H6)		0.0352	0.1881			
		0.0332	0.2013			
σ^*(S–H5)		0.0306	0.2455		0.0525	0.2778
		0.0309	0.2494		0.0536	0.2823
σ^*(O7–H8)					0.0460	0.2000
					0.0451	0.2099
σ^*(O9–H8)				0.0381		
				0.0383		
σ^*(O9–H6)					0.0604	0.1676
					0.0576	0.1631
$E^{(2)}$ ($\sigma \rightarrow \sigma^*$)/kJ mol^{-1}						
lp(N3) → σ^*(C–S)	322.2	3.6	5.9		2.8	2.2
	326.8[a)]	3.9	2.9		2.5	2.3
lp(S) → σ^*(C2–N3)	51.0	122.1	173.4			
	61.4	124.9	178.9			
lp(O7) → σ^*(S–H5)		33.8	597.5		68.8	728.9
		33.6	548.5		70.3	725.0
lp(N3) → σ^*(O9–H6)		56.8	377.9		108.2	333.1
		53.5	371.6		103.5	321.1
lp(S) → σ^*(O7–H5)	44.2			73.2		
	42.3			71.2		
lp(O9) → σ^*(N–H6)	43.5			74.1		
	44.5			77.0		
lp(O9) → σ^*(O7–H8)					93.2	443.0
					89.4	453.2
lp(O7) → σ^*(O9–H8)				72.7		
				73.2		

a) For species given in parenthesis. b) Natural charge of atoms in monomer H_2O.

charge-transfer energy associated with lp(S) → σ^*(C2–N3) interaction decreases upon **AW**(**CW**) dimerization. These interactions in **AW**(**CW**)-TSs are stronger than the corresponding interactions in **AW**(**CW**) complexes. In **AW**(**CW**) dimers, lp(S) → σ^*(O–H) and lp(O) → σ^*(N–H) intermolecular interactions are replaced by lp(O) → σ^*(S–H) and lp(N) → σ^*(O–H) interactions in **AW**(**CW**)-TSs which are stronger than those observed in ground states. In **AW**(**CW**) dimers, our results show that there are an increase in the σ^* population of the O–H and N–H bonds upon dimerization.

A comparison of the natural charge of atoms in free **A**(**C**) and **W** with **AW**(**CW**) complexes in Tables 5 and 6 shows that the charge transfer in complexes occurs from **A**(**C**) to **W**. The overall charge transfer from **A**(**C**) to **W** is 0.0179 (0.0165 au). As it can be seen in Table 6, complex formation of **AW**(**CW**) results in an increase of the electronic charge of S atom and the decrease of electronic charge of C2 atom. Therefore, polarity of C–S bond increases upon complex formation. This is as expected from elongation of the bond length upon complex formation and decrease of electronic density of C=S BCP which has been discussed in section AIM. Both C and S atoms lose electronic charge on going from **AW**(**CW**) to **AW**(**CW**)-TS. Our results show that the hydrogen atoms of the OH and NH lose electronic charges upon complexation. The decrease of the natural charge on H6 involved in NH···O interaction is smaller than that of H5 involved in OH···S interaction. Besides, H atoms in NH···O interaction losing electronic charge and N atoms gaining electronic charge in the **AW**(**CW**) to **AW**(**CW**)-TS process. In contrast, the O atoms in **AW**(**CW**) complexes lose electronic charge and H atoms in SH5···O interactions gain them on going from **AW**(**CW**) to **AW**(**CW**)-TS.

From Table 6, lp(S) → σ^*(O7–H5), lp(O7) → σ^*(O9–H8), and lp(O9) → σ^*(N–H) interactions play more a important role in stabilization of the **A2W**(**C2W**) complexes. These interactions are replaced by stronger interactions of lp(O7) → σ^*(S–H5), lp(O8) → σ^*(O7–H8), and lp(N) → σ^*(O9–H6) in transition states, in agreement with the stronger hydrogen bond predicted in transition states with respect to the those of ground states. The changes in the natural charge of atoms involved in HBs are similar to those found in **AW**(**CW**) to **AW**(**CW**)-TS process.

Conclusion

The present work deals with the effect of hydration and self-association on the reaction mechanism of proton transfer in methimazole (3-methyl-1*H*-imidazole-2(3*H*)-thione) and 1*H*-imidazole-2(3*H*)-thione by using quantum chemical calculations at the B3LYP/6-311++G(2d,2p) level of theory. On the basis of the results obtained from our calculations, the following can be stated: (1) The stability of complexes decreases in the order of **CC** > **AA** > **DD** > **BB**. Dimers **BB** and **DD** exhibit two S–H···N–C hydrogen bonds and dimers **AA** and **CC** represent two N–H···S–C type hydrogen bonds. As a result, stability of dimers increases with the increment of the number of H···S type hydrogen bonds. (2) The hydrogen-bond interaction in the self-assisted complexes **AA**(**CC**) is stronger than in water-associated complexes **A**(**C**)**W**. (3) For direct tautomerization to take place, **A**(**C**) must undergo large structural changes which are energetically expensive. Such geometric variations make the proton transfer difficult. (4) As a result, the lower energy barrier for **AA**(**CC**) → **AA**(**CC**)-TS, **A**(**C**)**W** → **A**(**C**)**W**-TS, and **A**(**C**)**2W** → **A**(**C**)**2W**-TS processes can be attributed to the smaller deformation of structure of monomers **A** and **C** in these processes with respect to **A**(**C**) → **A**(**C**)-TS) processes. (5) Direct transition is more difficult than the water-assisted and self-assisted processes both thermodynamically and dynamically. (6) The small negative value of $H(r)$ reveals some contribution of sharing interaction (partially covalent) to the S···HN bond. (7) AIM data reveal the partially covalent nature of S···H5 interaction and electrostatic nature of O···H6 interaction in **A**(**C**)–**W** complexes. (8) The negative $H(r)$ values for HBs increase on going from ground state to transition state. This indicates that the HBs for transition states are stronger than ground states. (9) In the present dimers, our results show that there is an increase in the σ^* population of the N–H bond in **A**(**C**) and O–H bond in **W** upon dimerization. (10) The weak HBs in ground states are replaced by strong HBs in transition states.

References

1 C. Laurence, M. J. El Ghomari, M. Lucon, *J. Chem. Soc., Perkin Trans. 2* **1998**, 1159.

2 C. Laurence, M. J. El Ghomari, M. Berthelot, *J. Chem. Soc., Perkin Trans. 2* **1998**, 1163.

3 C. Laurence, M. J. El Ghomari, J. Y. Le Questel, M. Berthelot, R. Mokhlisse, *J. Chem. Soc., Perkin Trans. 2* **1998**, 1545.

4 R. P. Lang, *J. Am. Chem. Soc.* **1962**, *84*, 1185.

5 R. P. Lang, *J. Phys. Chem.* **1968**, *72*, 2129.

6 A. F. Grand, M. Tarmes, *J. Phys. Chem.* **1970**, *74*, 208.

7 A. Suszka, *J. Chem. Soc., Perkin Trans. 2* **1985**, 531.

8 H.-J. Zhu, Y. Ren, J. Ren, S.-Y. Chu, *THEOCHEM* **2005**, *730*, 199.

9 G. A. Jeffrey, W. Saenger, *Hydrogen Bonding in Biological Structures*, Springer, Berlin, **1991**.

10 G. R. Desiraju, T. Steiner, *The Weak Hydrogen Bond in Structural Chemistry and Biology*, Oxford University Press, New York, **1999**.

11 A. Suszka, *J. Chem. Soc., Perkin Trans. 2* **1985**, 531.

12 A. Vila, R. A. Mosquera, *Int. J. Quantum Chem.* **2006**, *106*, 928, and references cited therein.

13 a) R. F. W. Bader, *Atoms in Molecules. A Quantum Theory*, Clarendon, Oxford, U.K., **1990**. b) R. F. W. Bader, *Chem. Rev.* **1991**, *91*, 893.

14 A. E. Reed, L. A. Curtiss, F. Weinhold, *Chem. Rev.* **1988**, *88*, 899.

15 M. J. Frisch, G. W. Trucks, H. B. Schlegel, G. E. Scuseria, M. A. Robb, J. R. Cheeseman, V. G. Zakrzewski, J. A. Montgomery, Jr., R. E. Stratmann, J. C. Burant, S. Dapprich, J. M. Millam, A. D. Daniels, K. N. Kudin, M. C. Strain, O. Farkas, J. Tomasi, V. Barone, M. Cossi, R. Cammi, B. Mennucci, C. Pomelli, C. Adamo, S. Clifford, J. Ochterski, G. A. Petersson, P. Y. Ayala, Q. Cui, K. Morokuma, D. K. Malick, A. D. Rabuck, K. Raghavachari, J. B. Foresman, J. Cioslowski, J. V. Ortiz, A. G. Baboul, B. B. Stefanov, G. Liu, A. Liashenko, P. Piskorz, I. Komaromi, R. Gomperts, R. L. Martin, D. J. Fox, T. Keith, M. A. Al-Laham, C. Y. Peng, A. Nanayakkara, C. Gonzalez, M. Challacombe, P. M. W. Gill, B. Johnson, W. Chen, M. W. Wong,

J. L. Andres, C. Gonzalez, M. Head-Gordon, E. S. Replogle, J. A. Pople, *Gaussian 98, Revision A.7*, Gaussian, Inc., Pittsburgh PA, **1998**.

16 A. D. Becke, *J. Chem. Phys.* **1993**, *98*, 5648.

17 C. Lee, W. Yang, R. G. Parr, *Phys. Rev. B* **1988**, *37*, 785.

18 P. R. Rablen, J. W. Lockman, W. L. Jorgensen, *J. Phys. Chem. A* **1998**, *102*, 3782.

19 J. J. Novoa, C. Sosa, *J. Phys. Chem.* **1995**, *99*, 15837.

20 D. R. Hamann, *Phys. Rev. B* **1997**, *55*, R10157.

21 C. Maerker, P. v. R. Schleyer, K. R. Liedl, T.-K. Ha, M. Quack, M. A. Suhm, *J. Comput. Chem.* **1997**, *18*, 1695.

22 K. Raghavachari, G. W. Trucks, J. A. Pople, M. Head-Gordan, *Chem. Phys. Lett.* **1989**, *157*, 479.

23 A. Fu, H. Li, D. Du, Z. Zhou, *J. Phys. Chem. A* **2005**, *109*, 1468.

24 F. Biegler-König, J. Schönbohm, D. Bayles, *J. Comput. Chem.* **2001**, *22*, 545.

25 a) P. Hobza, Z. Havlas, *Chem. Rev.* **2000**, *100*, 4253, and references cited therein. b) P. Hobza, V. Spirko, H. L. Selzle, E. W. Schlag, *J. Phys. Chem. A* **1998**, *102*, 2501.

26 a) M. T. Carroll, C. Chang, R. F. W. Bader, *Mol. Phys.* **1988**, *63*, 387. b) M. T. Carroll, R. F. W. Bader, *Mol. Phys.* **1988**, *65*, 695.

27 S. Vijayakumar, P. Kolandaivel, *J. Mol. Struct.* **2005**, *734*, 157.

28 U. Koch, P. L. A. Popelier, *J. Phys. Chem.* **1995**, *99*, 9747.

29 P. L. A. Popelier, *J. Phys. Chem. A* **1998**, *102*, 1873.